J. Am. Chem. Soc. 1987, 109, 56-61

Ultrahigh Resolution NMR. 6. Observation of Resolved ^{13}C–^{15}N Scalar Splittings in Carbon-13 NMR Spectra of Samples of Natural Isotopic Composition

Steven R. Maple and Adam Allerhand*

Contribution from the Department of Chemistry, Indiana Univeristy, Bloomington, Indiana 47405. *Received June 9, 1986*

Abstract: Ultrahigh resolution NMR spectroscopy yields resolved satellites from one-bond and long-range ^{13}C–^{15}N scalar coupling in ^{13}C NMR spectra of samples of natural isotopic composition, even though the natural abundance of ^{15}N is only 0.37% and $J(^{13}\mathrm{C}-^{15}\mathrm{N})$ values are typically in the range 1 to 10 Hz. All possible ^{13}C–^{15}N satellites are resolved in ^{13}C NMR spectra of pyridine and 2,6-dimethylpyridine, recorded with single-pulse excitation at 50.3 MHz in 10-mm sample tubes. As a bonus, each spectrum also yields secondary ^{15}N isotope effects (relative to ^{14}N) on ^{13}C chemical shifts, estimates of ^{14}N scalar contributions to the line widths of the major ^{13}C resonances, values of one-bond and long-range ^{13}C–^{13}C scalar coupling constants, and secondary ^{13}C isotope effects (relative to ^{12}C) on ^{13}C chemical shifts. Possible applications are discussed.

In recent reports,[1-5] we demonstrated the feasibility of achieving an instrumental contribution to the line width of less than 10 mHz in proton-decoupled ^{13}C NMR spectra on standard commercial NMR instruments, with the use of large (3-4 mL) sample volumes. This development has allowed the observation of resolved satellites from long-range ^{13}C–^{13}C scalar coupling in ordinary (single-pulse) ^{13}C Fourier transform NMR spectra of samples of natural isotopic composition, even though these satellites are very weak (0.55% of the intensity of the main peaks) and are typically only 0.5-5 Hz from the main peaks. In this report we show that, as a result of very recent improvements in the line shape,[5] ultrahigh resolution NMR permits the observation of resolved satellites from one-bond and long-range ^{13}C–^{15}N scalar coupling in ^{13}C NMR spectra of samples of natural isotopic composition, even though these satellites have only 0.185% (1/540) of the intensity of the corresponding main resonances, and in spite of the fact that the line widths of the main resonances may exhibit substantial broadening from ^{13}C–^{14}N scalar relaxation. We use pyridine (**1**) and 2,6-dimethylpyridine (**2**) as test molecules to show that a single ultrahigh resolution ^{13}C NMR spectrum of a sample of natural isotopic composition may actually yield the following information: (i) all or most one-bond and long-range ^{13}C–^{15}N scalar coupling constants; (ii) all or most ^{15}N (relative to ^{14}N) isotope effects on ^{13}C chemical shifts; (iii) values of ^{13}C–^{14}N scalar contributions to the line widths of the main resonances and estimates of ^{14}N relaxation times; (iv) all one-bond and all or most long-range ^{13}C–^{13}C scalar coupling constants; (v) one-bond and long-range ^{13}C isotope effects on ^{13}C chemical shifts.

Values of one-bond and long-range ^{13}C–^{15}N coupling constants have a variety of possible structural applications.[6] As far as we know, all previously reported values[6,7] were obtained with the use of ^{15}N-enriched compounds. The ability of ultrahigh resolution NMR to extract $J(^{13}\mathrm{C}-^{15}\mathrm{N})$ values from spectra of samples of natural isotopic composition greatly enhances the potential applications of these parameters.

Table I. Absolute Values of ^{13}C–^{15}N and ^{13}C–^{13}C Scalar Coupling Constants (Hertz) in **1**[a]

coupled nucleus[c]	observed carbon[b]		
	2	3	4
1[d]	0.729	2.515	3.802
2		54.21[e]	2.867
3	54.200		53.657
4	2.868	53.66[e]	
5	13.942[f]	*g*	*h*
6	*g*	13.943[f]	*i*

[a] Obtained from the spectrum shown (in part) in Figure 1. Estimated precision is ±0.002 Hz, except where indicated otherwise. [b] The carbon whose resonance yielded the observed satellites. [c] The nucleus (^{13}C or ^{15}N) which is coupled to the observed one. [d] Nitrogen-15. [e] Estimated precision is ±0.01 Hz because of partial overlap of the upfield satellites arising from C-2 and C-4 in the C-3 spectral region. [f] Coupling of C-2 with C-5 is structurally equivalent to coupling of C-3 with C-6. [g] Scalar coupling causes no splitting because the two coupled ^{13}C nuclei have identical chemical shifts. [h] See observed C-4 coupled to C-3. [i] See observed C-4 coupled to C-2.

Experimental Section

Each sample of **1** and **2** contained 40% v/v acetone-d_6. Proton-decoupled ^{13}C NMR spectra were recorded at 50.3 MHz and 26.5 °C on a slightly modified[2,5] Nicolet NT-200 NMR spectrometer equipped with a 10-mm probe from Cryomagnet Systems, Inc.[5] Spinning sidebands were smeared out by spinner speed modulation.[8] Line widths and relative peak positions were obtained with the use of a Lorentzian line-shape fit for all experimental points above half-height plus one more on each side of the peak. Spin-lattice relaxation times were measured essentially as described elsewhere.[2]

The spectrum of **1** was recorded with a digital resolution of 13.6 mHz. Other details are given in the legend of Figure 1. In the case of **2**, the data acquisition memory of 256K in our Nicolet 1280 computer would not have yielded the high digital resolution we desired for this feasibility study. Therefore, three separate narrow spectral widths were used for the C-2, C-3 plus C-4, and CH$_3$ regions, with digital resolution of 4.6, 19.6, and 18.3 mHz, respectively. Other details are given in the legends of Figures 2 and 3.

Results and Discussion

Our discussion is facilitated by arbitrarily setting to zero the frequency of each of the large resonances which arise from molecules which have ^{14}N plus a single ^{13}C nucleus. Figures 1 and 2 show the regions of ±2.5 Hz of the aromatic carbon resonances of **1** and **2**, respectively. Figure 3A shows the ±6 Hz region of the methyl resonance of **2**. The spectra of **2** were processed without any digital line broadening or narrowing, and they illustrate the actual resolution of the instrument. However, the spectrum of **1** shown in Figure 1 was processed with 40-mHz Lorentzian line *narrowing* plus 40-mHz Gaussian line *broadening*,[9]

---

(1) Allerhand, A.; Addleman, R. E.; Osman, D. *J. Am. Chem. Soc.* **1985**, *107*, 5809-5810.

(2) Allerhand, A.; Dohrenwend, M. *J. Am. Chem. Soc.* **1985**, *107*, 6684-6688.

(3) Allerhand, A.; Addleman, R. E.; Osman, D.; Dohrenwend, M. *J. Magn. Reson.* **1985**, *65*, 361-363.

(4) Maple, S. R.; Allerhand, A. *J. Magn. Reson.* **1986**, *66*, 168-171.

(5) Allerhand, A.; Bradley, C. H. *J. Magn. Reson.* **1986**, *67*, 173-176.

(6) Witanowski, M.; Stefaniak, L.; Webb, G. A. *Annu. Rep. NMR Spectrosc.* **1981**, *11B*, 1-486.

(7) Martin, G. J.; Martin, M. L.; Gouesnard, J.-P. *^{15}N-NMR Spectroscopy*; Springer-Verlag: Berlin, 1981.

(8) Bammel, B.; Evilia, R. F. *Anal. Chem.* **1980**, *52*, 1999-2000.

(9) Ferrige, A. G.; Lindon, J. C. *J. Magn. Reson.* **1978**, *31*, 337-340.

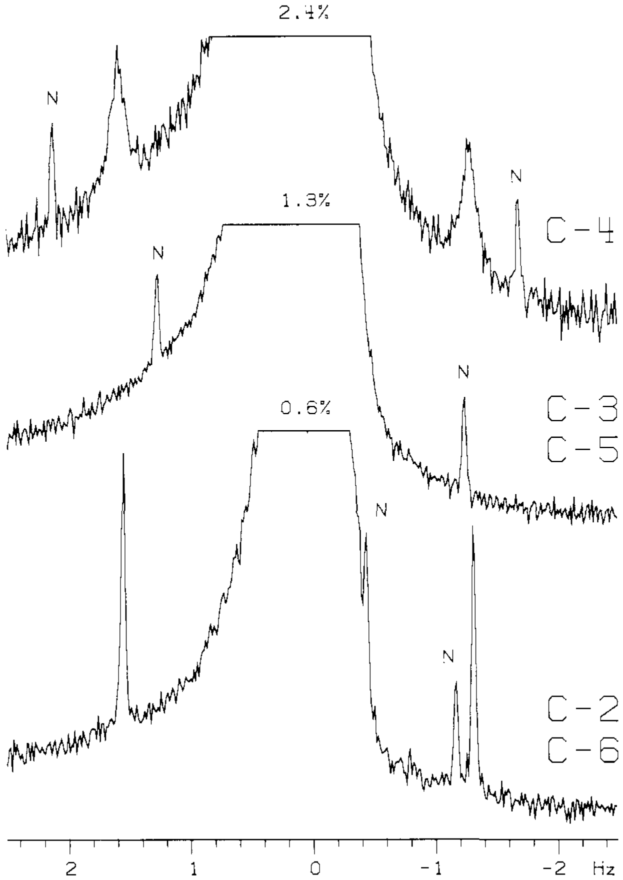

Figure 1. Regions of ±2.5 Hz relative to the major resonances in the proton-decoupled ^{13}C NMR spectrum of **1** (with 40% v/v acetone-d_6), recorded at 50.3 MHz and 26.5 °C, with an acquisition time of 36.83 s, a spectral width of ±889.679 Hz (quadrature detection), 128K time-domain data points, and 240 scans. The data were processed with 40-mHz Lorentzian narrowing plus 40-mHz Gaussian broadening. Fourier transformation was done after adding 128K "zero fill" time-domain data points, which yielded a digital resolution of 13.6 mHz. C-4 has a twofold vertical scale expansion relative to C-2 and C-3. Each main peak is truncated at the indicated percentage of its peak height. "N" designates $^{13}C-^{15}N$ satellites.

in order to improve the resolution of the ^{15}N satellite at −0.460 Hz in the region of C-2. All relative peak positions for **1** were obtained from the spectrum partially shown in Figure 1. However, line widths were measured from the corresponding spectrum processed without any digital line narrowing or broadening.

The ^{15}N satellites in the spectra of **1** and **2** were readily identified on the basis of their lower integrated intensities relative to those of the ^{13}C satellites. All expected $^{13}C-^{15}N$ and nearly all $^{13}C-^{13}C$ scalar splittings yielded resolved pairs of satellites. The resulting $^{13}C-^{15}N$ and $^{13}C-^{13}C$ coupling constants for **1** and **2** are given in Tables I and II, respectively. Our $J(^{13}C-^{15}N)$ values for **1** are in good agreement with reported values of lower precision.[10,11] Our $J(^{13}C-^{13}C)$ values for **1** are in good agreement with the reported one-bond coupling constants and the single reported long-range value.[12] We have not found any reported $J(^{13}C-^{15}N)$ or $J(^{13}C-^{13}C)$ values for **2**.

Because each $^{13}C-^{13}C$ pair yields two independently measured values for each $J(^{13}C-^{13}C)$, we can assign every satellite to a specific carbon–carbon pair, and we can also estimate the precision of the measurements by comparing the two $J(^{13}C-^{13}C)$ values obtained for each carbon–carbon pair. For all narrow and well-resolved resonances (the exceptions are indicated with a superscript *e* in Tables I and II), each pair of theoretically identical $J(^{13}C-^{13}C)$ values yields an experimental difference ≤0.002 Hz (see Tables I and II), which demonstrates the very high precision of chemical shift and coupling constant determinations made possible by ultrahigh resolution methodology.

Table II. Absolute Values of $^{13}C-^{15}N$ and $^{13}C-^{13}C$ Scalar Coupling Constants (Hertz) in **2**[a]

coupled nucleus[c]	observed carbon[b] 2	3	4	$CH_3(2)$
1[d]	1.018	2.596	2.401	9.776
2		56.598	1.858	51.27[e]
3	56.597		54.733	7.53[e]
4	1.859	54.731		*f*
5	11.815[g]	*h*	*i*	*j*
6	*h*	11.813[g]	*k*	5.63[e]
$CH_3(2)$	51.258	7.514	3.108	
$CH_3(6)$	5.669	*j*	*l*	*h*

[a] Obtained from the spectra shown (in part) in Figures 2 and 3. Estimated precision is ±0.003 Hz, except where indicated otherwise. $CH_3(2)$ and $CH_3(6)$ designate the methyl carbons bonded to C-2 and C-6, respectively. [b] The carbon whose resonance yielded the observed satellites. [c] The nucleus (^{13}C or ^{15}N) which is coupled to the observed one. [d] Nitrogen-15. [e] Estimated precision is ±0.02 Hz because of the large line widths of the ^{13}C satellites of the methyl carbon resonance (see text). [f] Satellites observed as shoulders on the main peak, because of the large line widths of the main methyl carbon resonance and its ^{13}C satellites (see text and Table V). [g] Coupling of C-2 with C-5 is structurally equivalent to coupling of C-3 with C-6. [h] Scalar coupling causes no splitting because the two coupled ^{13}C nuclei have identical chemical shifts. [i] See observed C-4 coupled to C-3. [j] Coupling of the methyl carbon to the aromatic carbon four bonds away did not yield resolved satellites. [k] See observed C-4 coupled to C-2. [l] See observed C-4 coupled to $CH_3(2)$.

Table III. Nitrogen-15 Isotope Effects (ppb) on the ^{13}C Chemical Shifts of **1** and **2**[a]

compd	$^1\Delta C(N)$	$^2\Delta C(N)$	$^3\Delta C(N)$
1	16.3	−0.1	−4.3
2	17.5	0.8[b]	−3.2

[a] Obtained from the spectra of Figures 1–3. We use here the notation of Hansen,[13] in which $^n\Delta X(Y)$ is an isotope effect, caused by two isotopes of nucleus Y, on the chemical shift of nucleus X, and *n* is the number of bonds which separate X and Y. The sign convention is to subtract the chemical shift of the molecule with the heavier isotope of Y from the corresponding value of the molecule with the lighter isotope. Estimated precision is ±0.1 and ±0.2 ppb for **1** and **2**, respectively. [b] This value refers to C-3. The $^2\Delta C(N)$ of the methyl carbon is 0.5 ppb.

We shall use the notation of Hansen,[13] described in footnote *a* of Table III, in our discussion of isotope effects on chemical shifts. A striking feature in the region of C-2 in the spectra of **1** and **2** (Figures 1 and 2, respectively) is that in each case *both* $^{13}C-^{15}N$ satellites are upfield of the major resonance, as a result of the relatively large $^1\Delta C(N)$ together with the relatively small value of $^1J(^{13}C-^{15}N)$ for C-2 (Tables I and II). Numerical values of $^n\Delta C(N)$ for all carbons of **1** and **2**, obtained from Figures 1 and 2, are presented in Table III. As a bonus, our spectra also yield one-bond and long-range ^{13}C isotope effects on the ^{13}C chemical shifts of **1** and **2**, given in Table IV. To ensure maximum accuracy of $^n\Delta C(C)$ values, we used the exact expressions for strong coupling of two spin-$^1/_2$ nuclei ("AB analysis")[14] to determine the chemical shifts of each component of a $^{13}C-^{13}C$ pair from the positions of the corresponding four observed peaks. It should be noted that the positions of the $^{13}C-^{13}C$ satellites of **2** came from three separate spectra of the regions of C-2, C-3 plus C-4, and CH_3 (see Experimental Section). Therefore, in order to carry out the AB analysis, it was also necessary to establish the relative chemical shifts of the three regions. The relative chemical shifts of the main resonances were obtained from

---

(10) Lichter, R. L.; Roberts, J. D. *J. Am. Chem. Soc.* **1971**, *93*, 5218–5224.

(11) Bundgaard, T.; Jakobsen, H. J. *Tetrahedron Lett.* **1976**, 1621–1624.

(12) Weigert, F. J.; Roberts, J. D. *J. Am. Chem. Soc.* **1972**, *94*, 6021–6025.

(13) Hansen, P. E. *Annu. Rep. NMR Spectrosc.* **1983**, *15*, 105–234.

(14) Harris, R. K. *Nuclear Magnetic Resonance Spectroscopy*; Pitman: London, 1983.

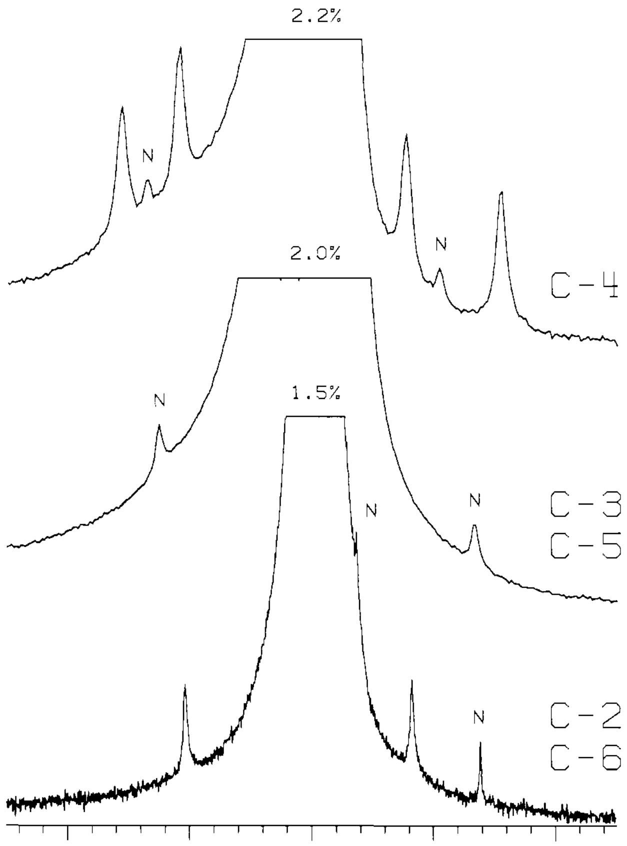

Figure 2. Regions of ±2.5 Hz relative to the major resonances in separate proton-decoupled ^{13}C NMR spectra recorded for the region of C-2 and that of C-3 plus C-4 of **2** (with 40% v/v acetone-d_6), at 50.3 MHz and 26.5 °C. In the following lists of parameters, the first number refers to the spectrum of C-2 and the second to that of C-3 plus C-4. The acquisition time was 109.18 and 25.56 s, the spectral width was ±150.060 and ±641.025 Hz (quadrature detection), the number of time-domain data points was 64K in both cases, and the number of scans was 140 and 520. No digital line narrowing or broadening was applied, and Fourier transformation was done after adding 64K "zero fill" time-domain data points, which yielded a digital resolution of 4.6 and 19.6 mHz. C-4 has a twofold vertical scale expansion relative to C-3. Each main peak is truncated at the indicated percentage of its peak height. "N" designates $^{13}C-^{15}N$ satellites.

a spectrum recorded with a width of ±6024.09 Hz and a digital resolution of 92 mHz. These chemical shift values were then used for the corresponding main peaks of Figures 2 and 3. The perils of the weak coupling approximation ("AX analysis")[14] is illustrated by considering the coupling of $^{13}CH_3$ to ^{13}C-2 in **2**. We obtained a chemical shift difference (at 50.3 MHz) of 6713.7 Hz and a coupling constant of 51.26 Hz, which yielded a ratio of 131, clearly a value normally considered in the "weak coupling" limit.[14] Nevertheless, an AX analysis yields chemical shifts for the ^{13}C-2 and $^{13}CH_3$ groups in error by about 0.1 Hz (2 ppb), a very large error in the context of $^n\Delta C(C)$ determinations (see Table IV). For pairs of aromatic carbons, the AX analysis yields large errors even for some long-range $^{13}C-^{13}C$ pairs.

Few $^1\Delta C(N)$ values, even fewer $^2\Delta C(N)$ values, and no $^3\Delta C(N)$ values have been reported. As far as we know, no $^n\Delta C(N)$ values have been reported for **1** and **2**. The magnitudes of our $^1\Delta C(N)$ and $^2\Delta C(N)$ values (Table III) are in the range of reported values for other compounds.[13] A limited number of $^1\Delta C(C)$[13,15] and a few $^2\Delta C(C)$[13,16-18] values have been reported, but not for **1** or **2**. Our $^1\Delta C(C)$ values of **1** and **2** are in the range 16.7–23.6 ppb, consistent with the range of about 10–30 ppb reported for other molecules.[13,15] A comparison of our data with $^n\Delta C(C)$ values is

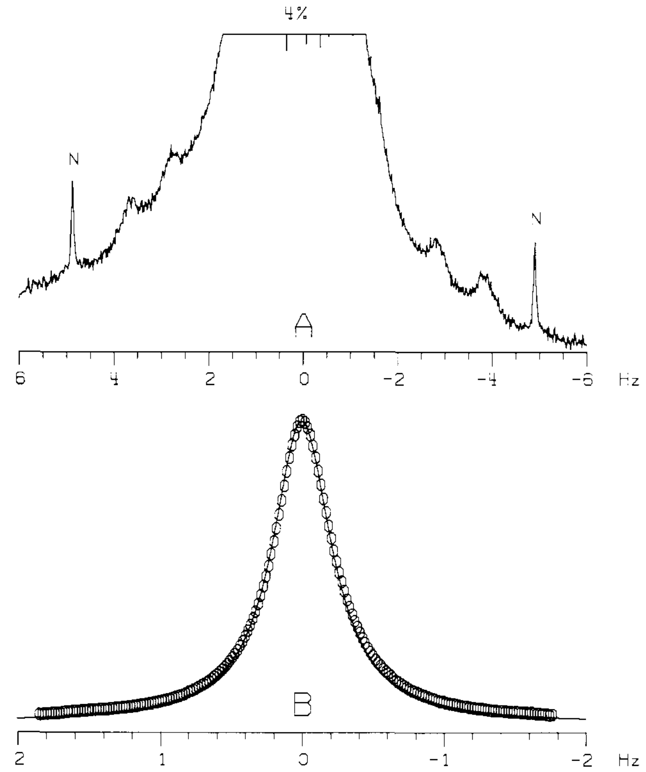

Figure 3. Proton-decoupled ^{13}C NMR spectrum of the methyl region of **2** (with 40% v/v acetone-d_6), recorded at 50.3 MHz and 26.5 °C, with an acquisition time of 27.28 s, a spectral width of ±300.300 Hz (quadrature detection), 32K time-domain data points, and 280 scans. No digital line narrowing or broadening was applied, and Fourier transformation was done after adding 32K "zero-fill" time-domain data points, which yielded a digital resolution of 18.3 mHz. (A) Region of ±6.0 Hz relative to the major peak, which is truncated at 4% of its peak height. "N" designates $^{13}C-^{15}N$ satellites. (B) Comparison of the experimental data points of the main peak (hexagons) with the best-fit Lorentzian curve to the top 29 points, which encompass the peak to just below half-height.

Table IV. Carbon-13 Isotope Effects (ppb) on the ^{13}C Chemical Shifts of **1** and **2**[a]

second ^{13}C	observed ^{13}C			
	2	3	4	$CH_3(2)$
2		23.6[b]	−3.0	*c*
		21.9	−3.4	5.7[d]
3	17.6		17.9	*c*
	18.9		17.3	2.1[d]
4	−2.0	17.2[b]		*c*
	−2.0	16.7		*e*
5	−3.8	*f*	*g*	*c*
	−2.9	*f*	*g*	*h*
6	*f*	−4.3	*i*	*c*
	f	−2.1	*i*	0.5[d]
$CH_3(2)$	*c*	*c*	*c*	
	6.3[d]	2.3[d]	*e*	
$CH_3(6)$	*c*	*c*	*c*	*c*
	0.1[d]	*h*	*j*	*f*

[a] Obtained from the spectra shown (in part) in Figures 1–3. In each case, the upper and lower values correspond to **1** and **2**, respectively. Estimated precision is ±0.1 ppb, except where indicated otherwise. [b] Estimated precision is ±0.2 ppb. [c] Not present in **1**. [d] Estimated precision is ±0.4 ppb. [e] The two $^{13}C-^{13}C$ satellites in the methyl carbon region were poorly resolved shoulders. Therefore, the AB quartet analysis (see text) was not feasible. [f] Scalar coupling causes no splitting because the two coupled ^{13}C nuclei have identical chemical shifts. [g] See observed C-4 coupled to C-3. [h] Coupling of the methyl carbon to the aromatic carbon four bonds away did not yield resolved satellites. [i] See observed C-4 coupled to C-2. [j] See observed C-4 coupled to $CH_3(2)$.

---

(15) Richarz, R.; Ammann, W.; Wirthlin, T. *J. Magn. Reson.* **1981**, *45*, 270–283.

(16) Nielsen, P. S.; Hansen, R. S.; Jakobsen, H. J. *J. Organomet. Chem.* **1976**, *114*, 145–155.

(17) Jokisaari, J. *Org. Magn. Reson.* **1978**, *11*, 157–159.

(18) Hansen, P. E.; Led, J. J. *Org. Magn. Reson.* **1981**, *15*, 288–293.

Table V. Experimental ^{13}C Line Widths, Estimated Contributions from ^{13}C–^{14}N Scalar Relaxation, and Estimated ^{14}N Line Widths

	1[a]			**2**[a]			
	C-2	C-3	C-4	C-2	C-3	C-4	CH_3
$1/\pi T_1$[b]	18	18	17	*c*	35	29	28
$W_{ex}(^{13}C-^{15}N)$[d,e]	*c*	52	50	*c*	60	55	52
$W_{ex}(^{13}C-^{15}N)$[e,f]	54	51	54	20	64	61	61
$W_{ex}(^{13}C-^{14}N)$[e,g]	52	109	176	25	100	97	504
W_Q[h]		58	124		38	39	448
$J(^{13}C-^{14}N)$[i]	520	1793	2710	726	1851	1712	6969
W_N[j]		150	160[k]		240	200	290[k]

[a] W_N is given in hertz. All other values are in millihertz. [b] Measured only for the major resonances. Estimated precision is ±5%. [c] Not measured. [d] Line width of the downfield ^{13}C–^{15}N satellite. [e] The values for **2** were obtained from the spectra shown in part in Figures 2 and 3. The values for **1** were obtained from the same time-domain data as Figure 1, but processed without any line broadening or narrowing. Estimated precision is ±5 mHz or ±5%, whichever is greater. [f] Line width of the upfield ^{13}C–^{15}N satellite. [g] Line width of the major resonance of the ^{14}N-containing molecule. [h] Contribution from ^{13}C–^{14}N scalar relaxation to the ^{13}C line width of the ^{14}N-containing molecule (see text). Estimated precision is ±10 mHz or ±10%, whichever is greater. [i] Absolute value of $J(^{13}C-^{14}N)$, taken as the corresponding $J(^{13}C-^{15}N)$ times 0.7129 (see text). [j] Line width of the ^{14}N resonance, computed from the values of W_Q and $J(^{13}C-^{14}N)$ of the carbon in this column (see text). [k] Estimated precision is ±10%. The other W_N values have lower precision (see text).

clouded by the limited accuracy of the earlier ones, which were obtained under conditions of lower resolution. This is particularly true for the few reported $^2\Delta C$(C) values,[16–18] which are in the range −12 to +10 ppb and have reported accuracies of ±3 ppb[16] and ±2 ppb.[17,18] Furthermore, there is also a problem in evaluating some published $^1\Delta C$(C) values which have a reported accuracy of ±10 ppb.[15] Although there is reason to believe that $^n\Delta C$(C) and $^n\Delta C$(N) values may have useful applications in structural studies,[13] the small number of reported values and the earlier difficulties in measuring them have probably conspired against systematic efforts to establish the applicability of these isotope effects in studies of molecular structure. This situation may now change because of the ability of ultrahigh resolution methodology to extract $^n\Delta C$(C) and $^n\Delta C$(N) values routinely from ^{13}C NMR spectra. However, many more $^n\Delta C$(C) and $^n\Delta C$(N) values will have to be measured, with the accuracy of the values of Tables III and IV, in order to establish their analytical and structural applications.

It is pertinent to discuss the experimental line widths (W_{ex}) of the ^{13}C resonances of **1** and **2**. Because of the very small instrumental contribution (W_{in}) to the line widths (see below), it is possible to make good estimates of the natural line width (W_0) for all but the narrowest resonances of **1** and **2**, as shown for other molecules in an earlier report.[2] The results are shown in Table V. It is evident that the ^{14}N-containing molecules exhibit much larger values of W_{ex} than the ^{15}N-containing ones, except for C-2. Note that the ^{13}C–^{13}C satellites are expected to have and do have essentially the same line-width values as those of the corresponding major resonances. Therefore, the large differences in W_{ex} between the ^{14}N- and ^{15}N-containing molecules shown in Table V are clearly observable in Figures 1–3, by comparing the resonances of the ^{13}C–^{13}C satellites with those of the ^{13}C–^{15}N satellites. The comparison is particularly dramatic for the methyl carbon region of **2** (Figure 3A), because the line widths of the two types of satellites differ by about a factor of 10. This can be readily explained on the basis of contributions to the line widths from ^{13}C–^{14}N scalar relaxation (W_Q).[19–24] The experimental line widths of Table V readily yield good estimates of W_Q, except for C-2 (see below).

The spin–lattice relaxation rate ($1/T_1$) of all ^{13}C resonances of **1** and **2**, except possibly C-2 of **2**, is certainly dominated by the ^{13}C–^{1}H dipolar mechanism.[25,26] It is possible that $1/T_1$ of C-2 of **2** has significant contributions from chemical shift anisotropy.[26] In any case, it is safe to assume that the ^{13}C T_1 values do not change when going from the measured ones for the major resonances (of the ^{14}N-containing molecules) to the corresponding T_1 values of the ^{13}C–^{15}N satellites. It is also safe to assume that the reciprocal of the rotational correlation time is much greater than the resonance frequency of 50.3 MHz (extreme narrowing limit).[25] In this case, we should have for all ^{13}C resonances of **1** and **2**

$$W_{ex}(^{13}C-^{15}N) = W_{in} + 1/\pi T_1 \quad (1)$$

$$W_{ex}(^{13}C-^{14}N) = W_{ex}(^{13}C-^{15}N) + W_Q \quad (2)$$

Here $1/\pi T_1$ is the measured ^{13}C spin–lattice relaxation rate (in Hz) of the ^{14}N-containing molecule, $W_{ex}(^{13}C-^{15}N)$ is the measured line width of the ^{13}C–^{15}N satellites (in Hz), $W_{ex}(^{13}C-^{14}N)$ is the corresponding value for the main resonance, and W_Q is the contribution from ^{13}C–^{14}N scalar relaxation to $W_{ex}(^{13}C-^{14}N)$.

Even though it is not needed for a determination of W_Q, it is of interest to estimate the instrumental contribution to the line widths, which can be done with the use of eq 1 and the values of $W_{ex}(^{13}C-^{15}N)$ and $1/\pi T_1$ in Table V. Clearly, W_{in} is about 30 mHz for proton-bearing carbons but less than 20 mHz for C-2 of **2**. These values are not much greater than the digital resolution in the corresponding spectra (see Experimental Section).

Equation 2 and the $W_{ex}(^{13}C-^{14}N)$ and $W_{ex}(^{13}C-^{15}N)$ values of Table V yield W_Q values also shown in Table V. We used the arithmetic average of the line widths of the upfield and downfield ^{13}C–^{15}N satellites for the $W_{ex}(^{13}C-^{15}N)$ required in eq 2. In the case of C-2, the contribution of W_Q is too small to yield a measurable difference between $W_{ex}(^{13}C-^{14}N)$ and $W_{ex}(^{13}C-^{15}N)$. An estimate of W_Q for C-2 can be made after an analysis of the data of the other carbons (see below). Values of 30 and 80 mHz have been reported for W_Q of C-3 and C-4, respectively, of **1** at 31 °C and slightly different solvent conditions from ours.[23] As expected, our values at 26.5 °C are larger. Our W_Q values, in conjunction with $J(^{13}C-^{14}N)$ computed from the corresponding $J(^{13}C-^{15}N)$ of Tables I and II by multiplying by the absolute value of the ratio of the gyromagnetic ratios of ^{14}N and ^{15}N (0.7129), can be used to estimate the ^{14}N relaxation times (T_{1N})[21,22,24] of **1** and **2**. We prefer to present instead the ^{14}N line widths (W_N), which in the extreme narrowing limit are given by $1/\pi T_{1N}$. It is useful to introduce the dimensionless parameter η defined by[19]

$$\eta = 10J/W_N \quad (3)$$

Here and for the rest of this discussion, J stands for $J(^{13}C-^{14}N)$. The scalar coupling of a spin-1 nucleus such as ^{14}N to a spin-$^1/_2$ nucleus will cause effects in the spectrum of the latter that depend strongly on η.[19–24] If $\eta >> 1$, the spin-$^1/_2$ resonance is split into three peaks, while if $\eta << 1$, a single peak is observed.[19,20] The analysis is simplest in these two limiting cases, which yield essentially Lorentzian line shapes.[19,20] On the basis of reported W_N values for **1**[21,24,27] and **2**[24] (although at different temperatures and in different solvents than our studies), we can expect a W_N in the range 150–300 Hz for **1** and **2** under our experimental conditions. On this basis, the largest value of η, that of the CH_3 of **2**, should be in the range 0.2–0.5. It has been implied[21] that such values are outside the range of validity of the simple "fast exchange" equation for $\eta << 1$ and that one must use cumbersome "intermediate exchange" equations[21,24] instead. Because this

---

(19) Pople, J. A. *Mol. Phys.* **1958**, *1*, 168–174.
(20) Suzuki, M.; Kubo, R. *Mol. Phys.* **1963**, *7*, 201–209.
(21) Kintzinger, J. P.; Lehn, J. M. *Mol. Phys.* **1986**, *14*, 133–145.
(22) Cunliffe, A. V.; Harris, R. K. *Mol. Phys.* **1968**, *15*, 413–422.
(23) Hansen, M.; Jakobsen, H. J. *J. Magn. Reson.* **1973**, *10*, 74–84.
(24) Lehn, J. M.; Kintzinger, J. P. In *Nitrogen NMR*; Witanowski, M., Webb, G. A., Eds.; Plenum: New York, 1973; Chapter 3.
(25) Allerhand, A.; Doddrell, D.; Komoroski, R. *J. Chem. Phys.* **1971**, *55*, 189–198.
(26) Norton, R. S.; Clouse, A. O.; Addleman, R.; Allerhand, A. *J. Am. Chem. Soc.* **1977**, *99*, 79–83.
(27) Witanowski, M.; Stefaniak, L.; Januszewski, H. *Tetrahedron Lett.* **1971**, 1653–1656.

misconception (see below) seems to have propagated in the literature,[23] we shall proceed to dispel it and then use the "fast exchange" limit.

Cunliffe and Harris[22] reported detailed studies of the line shape of a spin-$^1/_2$ coupled to a spin-1. They showed that for $\eta \lesssim 2$ the observed *single resonance* has a line shape which does not show detectable deviations from Lorentzian. We used the "intermediate exchange" equation of Kintzinger and Lehn[21] to compute the value of W_Q for $\eta = 1$. The result differed by about 0.3% from the one obtained from the "fast exchange" equation[14,24]

$$W_Q = (8/3)J^2/W_N \qquad (4)$$

Therefore, we used eq 4 for estimating W_N from the values of W_Q and J of Table V. The resulting W_N for **1** and **2** are also shown in Table V.

Figure 3B shows the experimental line shape of the CH_3 resonance of **2** (hexagons) together with the best-fit Lorentzian curve. Clearly, as expected from the above discussion, the experimental line shape is very well represented by a Lorentzian. Please note that the observed line shape is essentially the *natural* one, because the instrumental contribution is only about 30 mHz (out of a total of about 500 mHz) at half-height, and only about 0.5 Hz (out of about 6 Hz) at 0.5% intensity.[5]

Our ^{13}C line widths yield two values for W_N of **1** and three values for W_N of **2** (Table V). Obviously, under conditions of no experimental error all W_N values determined for a single molecule should be identical. The two values for **1** differ by only 7%. However, the lowest and highest ones for **2** differ by 45%, and the two smallest ones differ by 20%. These large discrepancies must be the result of large errors in the rather small values of W_Q of C-3 and C-4 (given as 38 ± 10 and 39 ± 10 mHz, respectively, in Table V). The W_Q of the CH_3 (450 ± 45 mHz) should yield the most accurate W_N. In the case of **1**, C-4 has a W_Q twice as large as that of C-3, so that the W_N based on C-4 should be more accurate than the one from C-3. Our best W_N values of 160 and 290 Hz for **1** and **2**, respectively, are consistent with reported values for **1**[21,24,27] and **2**[24] in different solvents and at different temperatures. The W_N value of **2** is about 80% larger than that of **1**. The value of W_N should be proportional to the rotational correlation time and the square of the ^{14}N quadrupole coupling constant.[14] Although we have not found a reported quadrupole coupling constant for **2**, a comparison of the values for **1** and several methyl-substituted derivatives of **1**[24] suggests that the ^{14}N quadrupole coupling constants of **1** and **2** should differ by no more than about 10%. Therefore, the larger W_N of **2** must be caused mainly by a longer rotational correlation time than that of **1**. This conclusion is consistent with the fact that the $1/\pi T_1$ values of the methine aromatic carbons of **2** are about 80% larger than the corresponding ones of **1** (Table V).

If we introduce into eq 4 the W_N value of **1** or **2** and the corresponding $J(^{13}C-^{14}N)$ of C-2, we obtain W_Q values of 4.5 and 4.8 mHz for C-2 of **1** and **2**, respectively. These small W_Q values are consistent with the unmeasurable difference between $W_{ex}(^{13}C-^{14}N)$ and $W_{ex}(^{13}C-^{15}N)$ for C-2. It is fortuitous that the observed difference for C-2 of **2** is 5 mHz (Table V).

Concluding Remarks

Under conditions of ultrahigh resolution and large signal-to-noise ratios, a *single* natural-abundance proton-decoupled ^{13}C NMR spectrum yields not only the chemical shifts of the main peaks but also a cornucopia of other spectroscopic data. Values of one-bond and long-range $J(^{13}C-^{13}C)$ and $J(^{13}C-^{15}N)$ which are larger than about 1 Hz can be measured with an accuracy of ±0.002 to ±0.02 Hz when the line widths are in the range 0.05–0.5 Hz. Values of $^n\Delta C(C)$ and $^n\Delta C(N)$ as small as 0.5 ppb (0.0005 ppm in units more familiar to NMR practitioners) can be measured with an accuracy of 0.2 ppb or better. Natural line widths (W_0) greater than about 0.1 Hz can be measured with increasing accuracy as they get larger, which allows rapid measurement of accurate spin–spin relaxation times (T_2). It must be emphasized that the possible applications of $J(^{13}C-^{13}C)$, $J(^{13}C-^{15}N)$, $^n\Delta C(C)$, $^n\Delta C(N)$, and W_0 are made more attractive by the fact that it is not necessary to record separate series of spectra for chemical shifts, coupling constants, isotope effects on chemical shifts, and spin–spin relaxation times. All of them are contained in a single ordinary "one-pulse" Fourier transform NMR spectrum. The great potential of easy ^{13}C T_2 measurements is implicitly contained in the vast literature on past applications of ^{13}C T_1 values. The possible structural applications of $J(^{13}C-^{13}C)$ are also well documented,[28] and there is some evidence for applications of $J(^{13}C-^{15}N)$ to structure determination.[6] However, extensive data tabulations need to be generated in order to establish how useful $^n\Delta C(C)$ and $^n\Delta C(N)$ values can be. As a first step, we have shown here that such tabulations can now be generated rapidly without chemical synthesis of ^{13}C-labeled and ^{15}N-labeled compounds. Table III suggests that $^n\Delta C(N)$ values may be usable to establish carbon–*nitrogen* connectivities in molecules, because it appears that $^1\Delta C(N)$ has relatively large positive values, while $^2\Delta C(N)$ and $^3\Delta C(N)$ have small positive or negative values. In the past, carbon–*carbon* connectivities have been established from $^1J(^{13}C-^{13}C)$ values[15] obtained by means of one-dimensional double-quantum-coherence ^{13}C NMR spectra,[29] or from two-dimensional double-quantum-coherence methods[30,31] which do not yield $^1J(^{13}C-^{13}C)$ but do depend on their values. In both methods the validity of the resulting carbon–carbon connectivities rests on the generally valid rule that $^1J(^{13}C-^{13}C)$ values are much larger than long-range $^{13}C-^{13}C$ coupling constants.[28] No such rule exists for $J(^{13}C-^{15}N)$ values,[6] as can be seen in Table I and II. Therefore, carbon–nitrogen connectivities do not follow readily from $J(^{13}C-^{15}N)$ values, so that the possibility of using $^n\Delta C(N)$ values for this purpose is particularly attractive. Even for carbon–carbon connectivities, the $J(^{13}C-^{13}C)$ methods may fail for some molecular structures which contain a carbonyl group and chlorine atoms, in which $^2J(^{13}C-^{13}C)$ values can be as large or larger than $^1J(^{13}C-^{13}C)$.[32] Not enough $J(^{13}C-^{13}C)$ values have been reported to exclude the possibility of many other instances of anomalously large long-range $J(^{13}C-^{13}C)$ values, or perhaps anomalously small $^1J(^{13}C-^{13}C)$ values. Therefore, it is of interest to determine if $^n\Delta C(C)$ values can supplement the use of $^1J(^{13}C-^{13}C)$ in establishing carbon–carbon connectivities. The $^1\Delta C(C)$ values of Table IV range from +5.7 to +23.6 ppb, and most are greater than +15 ppb, while the $^n\Delta C(C)$ values (n = 2, 3) go from −4.3 to +2.3 ppb. It seems desirable to measure $^n\Delta C(C)$ in a variety of molecular structures in order to establish if these trends are general and therefore usable for carbon–carbon connectivity determinations.

In this feasibility study we have chosen to use very long data acquisition times per scan (37 s for **1**, and 109, 26, and 27 s for the spectra of C-2, C-3 plus C-4, and CH_3, respectively, of **2**), in order to obtain very high precision of numerical data. Much shorter times will still yield all or most of the data reported here, but at the expense of diminished precision. The high precision of Tables I–V is unnecessary for most applications. It is also of interest to establish minimum molar concentrations and practical upper limits of molecular size for future studies. We believe that a 1 M solution represents the lower limit for routine determinations of $J(^{13}C-^{15}N)$ and $^n\Delta C(N)$ on our instrument, although much lower concentrations will be practical on "300-MHz" and "500-MHz" (^1H frequency) instruments when such instruments become ultrahigh resolution spectrometers. Obviously, $J(^{13}C-^{13}C)$ and $^n\Delta C(C)$ values can be obtained with one-third the concentrations required for $J(^{13}C-^{15}N)$ and $^n\Delta C(N)$. The practical upper limit of molecular size is more difficult to establish precisely. It will depend both on the solubility required to reach the necessary

---

(28) Marshall, J. L. *Carbon-Carbon and Carbon-Proton NMR Couplings: Applications to Organic Stereochemistry and Conformational Analysis*; Verlag Chemie Int.: Deerfield Beach, FL, 1983.

(29) Bax, A.; Freeman, R.; Kempsell, S. P. *J. Am. Chem. Soc.* **1980**, *102*, 4849–4851.

(30) Bax, A.; Freeman, R.; Frenkiel, T. A. *J. Am. Chem. Soc.* **1981**, *103*, 2102–2104.

(31) Bax, A.; Freeman, R.; Frenkiel, T. A.; Levitt, M. H. *J. Magn. Reson.* **1981**, *43*, 478–483.

(32) Bauer, H.; Buddrus, J.; Auf der Heide, W.; Kimpenhaus, W. *Angew. Chem., Int. Ed. Engl.* **1985**, *24*, 854–855.

minimum concentration and on the maximum W_0 values that will yield resolved ^{13}C–^{13}C and ^{13}C–^{15}N satellites. It is clear from Figure 3 that a W_0 of as much as 0.5 Hz still permits the resolution of ^{13}C–^{15}N and even long-range ^{13}C–^{13}C satellites. Here the big advantage of ultrahigh resolution methodology is the elimination of the very large instrumental contributions to the line width at the 0.1–0.5% intensity range (of the major resonance).[5] Even for W_0 = 1 Hz, one should expect to resolve many ^{13}C–^{15}N and long-range ^{13}C–^{13}C satellites. Very many large and complex molecules of chemical and biological interest exhibit ^{13}C line widths of no more than about 1 Hz.[25]

Acknowledgment. This work was supported by grants from the National Science Foundation (PCM 83-04699) and the National Institutes of Health (GM 22620). We thank Mr. Robert E. Addleman and Mr. Deon Osman for their help in many ways.

Nondestructive Photoorientation by Generalized Pseudorotation: A Quantitative Treatment

Juliusz G. Radziszewski, Fritz A. Burkhalter, and Josef Michl*[†]

Contribution from the Department of Chemistry, University of Utah, Salt Lake City, Utah 84112. *Received June 23, 1986*

Abstract: A quantitative analysis is presented of the photooriented stationary state reached upon irradiation of matrix-isolated molecules capable of undergoing photoinduced pseudorotation or enantiomeric inversion between two forms related by mirroring in a symmetry plane, assuming negligible site memory effects. The photostationary orientation distribution is a simple function of the angle ω between the directions that the absorbing transition moment occupies in two forms. The lowest theoretical dichroic ratio d for the transition that is being pumped results for $\omega = \pi/2$ and equals 0.4. Experiments have been performed on octaethylporphine ($\omega = \pi/2$) in various rigid media; the lowest d value was observed in solid Ne at 3 K and equaled 0.46, revealing the absence of significant site memory effects. The potential of this type of measurement for the determination of UV and IR transition moment directions in matrix-isolated molecules and the potential usefulness of systems of this kind for erasable optical information storage are pointed out.

The anisotropic nature of polarized and/or collimated light can be used to achieve orientation of initially random molecular assemblies (photoorientation[1]). In sufficiently viscous media, such photoinduced orientation can be long-lived and can be exploited in various ways, from spectroscopic studies of the anisotropy of molecular properties to optical recording of information.

The orienting effect of light is due primarily to the interaction of its electric vector with permanent or induced molecular electric dipole moments. Presently, we focus attention on the photoorientation induced by the latter and due to the anisotropic nature of UV, visible, or IR light absorption. For a nondegenerate transition, the electric dipole absorption probability is proportional to $\cos^2 \delta$, where δ is the angle between the electric field direction Z of linearly polarized light and the molecular transition moment, whose position is fixed within the molecular framework. The orientation discriminating action of light is known as photoselection.[1-3]

Destructive photoorientation by photoselection on an originally random sample occurs for photolabile solutes. After partial photodestruction with Z-polarized light, the remaining solute molecules are partially oriented in that δ values close to $\pi/2$ are favored. The orientation is uniaxial with respect to Z and becomes perfect, with $\delta = \pi/2$, as the remaining amount of the original solute goes to zero.[3,4] The photoproduct is partially oriented as well, unless the phototransformation is accompanied by complete positional randomization. Photoproduct orientation is complementary to that of the remaining starting material and decreases with the increasing degree of conversion, finally disappearing when the photoconversion is complete.

Destructive photoorientation has been well-known for a long time and has found frequent use in molecular spectroscopy.[1-3] Cases in which the photoproduct is oriented and cases in which it is not have both been observed.[5]

Nondestructive photoorientation by photoselection on an originally random sample is possible in principle for solutes which are not bleached upon light absorption but has been observed to occur only rarely. This is unfortunate in view of its obvious advantages.

The simplest mechanism for nondestructive photoorientation by anisotropic absorption of Z-polarized light is photoinduced rotational diffusion. This should operate in principle for all solute molecules that convert at least some of the absorbed light energy into heat and a local decrease in viscosity. It should also yield perfect uniaxial orientation ($\delta = \pi/2$) in the limit of infinite irradiation time. However, it has apparently never been observed to produce an observable effect for molecules imbedded in frozen gas matrices, glasses, or polymers.[1] It is conceivable that a suitable choice of viscous solvent and of temperature may yet uncover the operation of this mechanism; evidence for enhanced translational diffusion upon nondestructive photoexcitation in 2-methyltetrahydrofuran glass ("internal melting") was reported some time ago.[6]

Successful nondestructive photoorientation has been reported in several instances in which molecular structural rearrangements are clearly at play, reproducing ultimately the initial solute molecule in a different orientation (orientation by photoinduced pseudorotation) or producing its enantiomer (orientation by photoinduced inversion). We shall refer to these two mechanisms jointly as photoorientation by generalized pseudorotation. Thus, certain metal carbonyls such as $Cr(CO)_5$ have been partially oriented in frozen gas matrices by a photoprocess believed to involve pseudorotation by motion of the CO ligands,[7] and various

---

[†] Present address: Department of Chemistry, University of Texas at Austin, Austin, TX 78712-1167.

(1) Albrecht, A. C. *J. Chem. Phys.* **1957**, *27*, 1413; *J. Mol. Spectrosc.* **1961**, *6*, 84.

(2) Dörr, F. In *Creation and Detection of the Excited State*; Lamola, A. A., Ed., Marcel Dekker: New York, 1971; Vol. 1, Chapter 2.

(3) Michl, J.; Thulstrup, E. W. *Spectroscopy with Polarized Light*; VCH: Deerfield Beach, FL, 1986.

(4) Deering, R. A.; Kraus, A. A., Jr.; Gray, D. M.; Kilkson, R. *J. Theor. Biol.* **1966**, *13*, 295.

(5) E.g.: Raabe, G.; Vančik, H.; West, R.; Michl, J. *J. Am. Chem. Soc.* **1986**, *108*, 671.

(6) Dvořák, V.; Michl, J. *J. Am. Chem. Soc.* **1976**, *98*, 1080.

(7) Burdett, J.; Turner, J. J. In *Cryochemistry*; Moskovits, M., Ozin, G. A., Eds.; Wiley-Interscience: New York, 1976; p 514.

0002-7863/87/1509-0061$01.50/0